المجلة العربية للعلوم والهندسة

MODIFIED FAILURE CRITERIA FOR SHALES

Musaed N. J. Al-Awad*

Petroleum Engineering Department
King Saud University
Riyadh, Saudi Arabia

and

B. G. D. Smart

Department of Petroleum Engineering
Heriot-Watt University
Edinburgh, UK

THE ARABIAN JOURNAL FOR SCIENCE AND ENGINEERING

REPRINT

Published by KING FAHD UNIVERSITY OF PETROLEUM AND MINERALS, DHAHRAN 31261, SAUDI ARABIA

MODIFIED FAILURE CRITERIA FOR SHALES

Musaed N. J. Al-Awad*

Petroleum Engineering Department
King Saud University
Riyadh, Saudi Arabia

and

B. G. D. Smart

Department of Petroleum Engineering
Heriot-Watt University
Edinburgh, UK

الخلاصة :

إن معظم الصخور الطينية (الطفل) والتي تحتوي على كميات معقولة من المعادن الطينية (مثل المونتمور إلينيت) سوف تمتص الراشح من طين الحفر (ماء + أيونات) مما يؤدي إلى عدم الثباتية فى البئر المحفورة . عندما تتلامس مع الراشح من طين الحفر ، فإنّ تلك الصخور الطينية سوف تنتفخ وينشأ نتيجة لذلك منطقة انتفاخ محيطة بالبئر المحفورة . وبذلك فإن الخواص الميكانيكية أو قوة الصخر فى منطقة الانتفاخ ستقل مما يتسبب فى حدوث مشاكل جمّة فى ثباتية البئر المحفورة مثل انحشار أنبوب الحفر ، وصعوبة سحب أنبوب الحفر ، ومشاكل أخرى عديدة . لذلك فإن الإجهادات الانتفاخية يجب أن تُوخذ بعين الاعتبار عند أية محاولة جدّية للتمثيل الرياضي والتنبؤ بالخواص الميكانيكية للصخور الطينية بعد التفاعل مع الراشح من طين الحفر . ولقد تّم فى هذه الدراسة تضمين الإجهادات الانتفاخية فى معادلة (موهر–كولمب) المشهورة لانهيارية الصخور ؛ وعليه فإنّ الشكل المطوّر لهذه المعادلة قد أُخذ بعين الاعتبار الخواص الميكانيكية الطبيعية للصخور الطينية وكذلك الإجهادات الانتفاخية المتولدة وأصبح من الممكن التنبؤ بقوة الصخر وخصائصه الميكانيكية بعد التفاعل مع الراشح من طين الحفر تحت ظروف قاع البئر . وتم التحقق من صحة تلك المعادلة المطورة معملياً .

*Address for correspondence:
Petroleum Engineering Department, College of Engineering
King Saud University
P.O. Box 800, Riyadh 11421
Saudi Arabia

ABSTRACT

Most shale rocks which contain an appreciable fraction of reactive clays (*e.g.* montmorillonite) will adsorb mud filtrate (water+ions) and cause unstable hole conditions. When contacted with the mud filtrate, these shales will swell, creating a soft, swollen zone around the wellbore, therefore, the natural mechanical properties or the strength of the swollen shales will decrease causing serious hole problems such as undergauge hole, stuck pipe, overpull on trips, and several other problems. Thus swelling stresses and rock strength reduction must be included in any attempt to effectively model shale mechanical properties after interaction with drilling fluid filtrate. In this study shale swelling stresses were integrated into the prominent Mohr–Coulomb failure criterion and therefore a new form of this criterion has been introduced which combined the natural mechanical properties with swelling stresses to predict the in-situ strength of shales when invaded by the drilling fluid filtrate. The modified failure criterion was verified experimentally.

MODIFIED FAILURE CRITERIA FOR SHALES

1. INTRODUCTION

The swollen zone created around the wellbore during drilling in shale sections will be driven inward by high overburden stresses and require that higher than usual mud weights be used to counteract this inward displacement [1]. When shale contains a high native water content, even before it is exposed to drilling fluid, it is abnormally weak and unable to withstand the differential stress imposed by drilling out the surrounding rock (support). The mode of failure, when the stress differential created by the relief of lateral stress exceeds the yield strength of the formation, is plastic deformation of the wellbore. If the shale is under abnormally high pore pressure, spalling will be the result [2]. Swelling stresses generated due to the interaction between the shale and water-based drilling fluids must be taken into account when predicting the effect of swelling on borehole stability and failure criterion [3].

2. FORMULATION OF THE MODIFIED FAILURE CRITERION

Mohr's strength theory is normally used to represent the strength of rocks subjected to compressive stresses (axial and confining) given in terms of total stresses by:

$$\tau_f = \tau_o + \sigma \tan(\phi) . \tag{1}$$

In addition, the concept of effective stress can be used to modify Equation (1) to the following form [4]:

$$\sigma^i_{\text{eff}} = \sigma^i - P_p , \tag{2}$$

$$\tau_f = \tau_o + \left(\sigma - P_p\right) \tan(\phi) . \tag{3}$$

As shown in Figure 1, the stress state is represented by Mohr's circle. On circle 1 the line which passes through point "A" gives the angle of obliquity of the resultant stress with the x-axis, as follows [5]:

$$\beta = \left[\frac{\tau - \tau_o}{\sigma}\right] . \tag{4}$$

Failure will occur when β increases to the maximum angle of obliquity ϕ. Circle 1 represents a dry rock ($\beta<\phi$) assuming the rock is fully saturated with water and is not subjected to a positive hydraulic pore pressure. An increase in pore pressure shifts Mohr's circle 1 to the left (circle 2) increasing β to its maximum value ϕ and failure will occur on the plane represented by τ_f. Bol *et al.* [6] have suggested that the dimensional effective stress relation for shale is as follows:

$$\sigma^i_{\text{eff}} = \sigma^i - P_p \pm \sigma^i_{\text{hyd}} . \tag{5}$$

By substituting Equation (5) into Equation (1) and accounting for the moisture adsorption–desorption process, Equation (1) can be rewritten as follows:

$$\tau_f = \tau_o + \left(\sigma - P_p \pm \sigma_{\text{hyd}}\right) \tan(\phi) . \tag{6}$$

The swelling (hydration) σ_{hyd} stress is composed of two major stresses called the osmotic swelling stress σ_{os} and the surface swelling stress σ_{sur}, therefore Equation (6) can be expanded as follows:

$$\tau_f = \tau_o + \left(\sigma - P_p \pm \left(\sigma_{os} + \sigma_{sur}\right)\right) \tan(\phi) . \tag{7}$$

Finally the pore pressure terms are combined with the swelling terms and defined as the total swelling stress. Therefore Equation (7) changes to:

$$\tau_f = \tau_o + (\sigma - \sigma_{ts}) \tan(\phi) . \tag{8}$$

Equation (8) represents the modified Mohr–Coulomb failure criterion for shales.

3. APPLICATION OF THE MODIFIED FAILURE CRITERION

The following points show how this model is applied to experimental data:

(*i*) Swelling stresses are assumed to develop in two directions [7, 8] firstly normal to bedding planes and secondly, parallel to bedding planes as shown in Figure 2:

σ_{ts}^{V} = the total swelling stress in the direction normal to bedding planes.

σ_{ts}^{H} = the total swelling stress in the direction parallel to bedding planes.

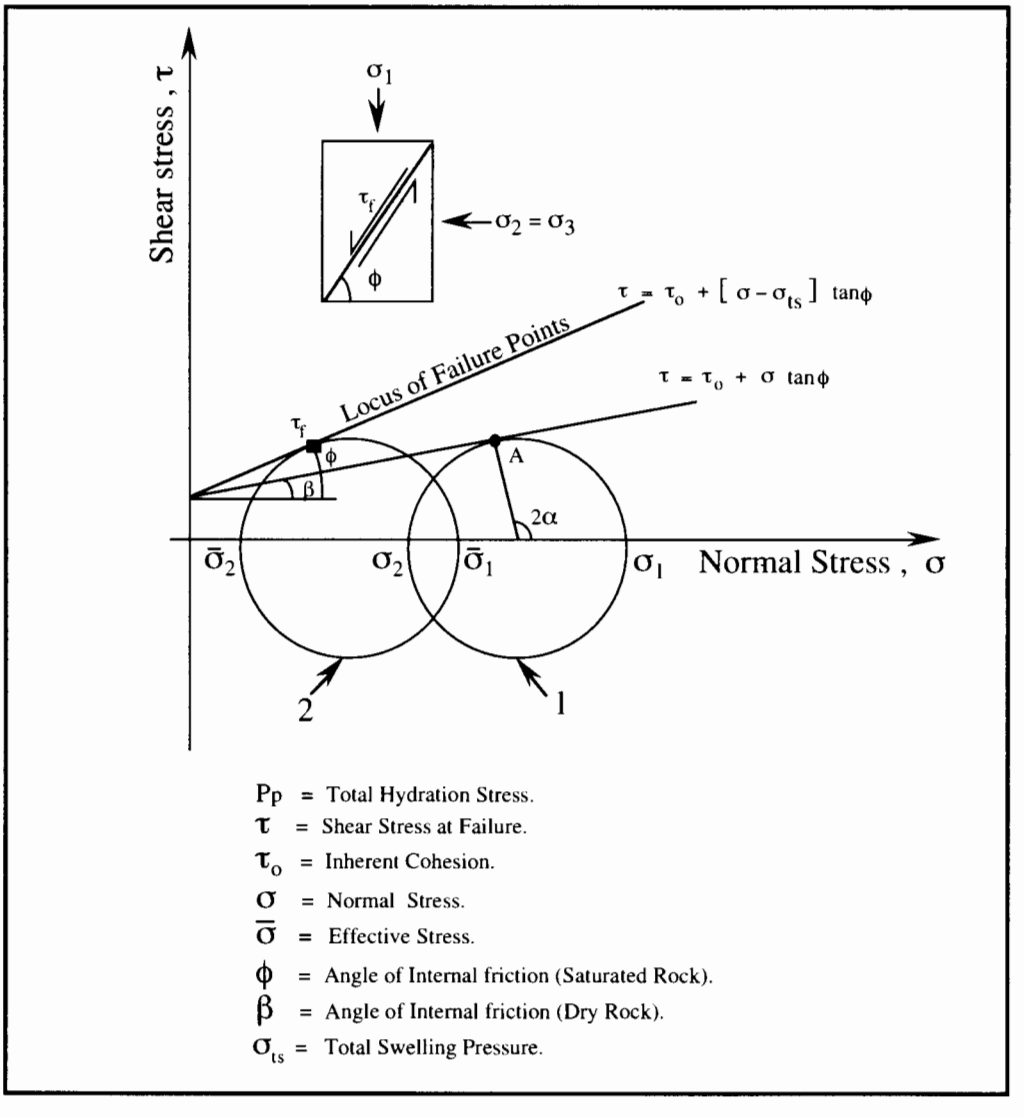

Figure 1. Shear Failure Criteria for Argillaceous Rocks With and Without Swelling (Pore Pressure) Effect.

(*ii*) Total swelling stresses are related to each other by the anisotropy factor [7, 8]:

$$F_{\text{anis}} = \left[\frac{\sigma_{\text{ts}}^{H}}{\sigma_{\text{ts}}^{V}}\right]. \tag{9}$$

(*iii*) Total swelling stresses are integrated into experimental triaxial compressive data as follows:

Axial stress at failure = $\sigma_1 - \sigma_{\text{ts}}^{V}$

Confining pressure at failure = $\sigma_3 - \sigma_{\text{ts}}^{H} = \sigma_3 - \left[F_{\text{anis}}\sigma_{\text{ts}}^{V}\right]$.

(*iv*) Confining pressures and axial stresses at failure are obtained from triaxial tests conducted on intact shale samples (zero moisture content) under realistic stresses.

(*v*) Total swelling stresses are obtained from tests conducted on cylindrical shale specimens under realistic stresses as shown in Section 4.5.

4. EXPERIMENTAL SET UP AND ANALYSIS OF TESTING MATERIALS

4.1. Analysis of Tested Shale

The shale used in this study was moderately hard, grey in color, and has an average specific gravity of 2.5. This shale was cored from an underground coal mine (Scotland, U.K.) from a depth between 250 to 270 meters. X-ray diffraction analysis has shown that this shale is composed of: 24% calcite and quartz, 3% montmorillonite, 13% illite, and 60% kaolinite.

4.2. Shale Anisotropy Factor

In this technique the shale were cut into cylindrical specimens, and strain gauges were attached diametrically opposed on the samples. The leads were connected and strain gauges coated with waterproof material. These strain gauges were arranged to measure swelling strains in both vertical and horizontal directions (normal and parallel to bedding planes). The samples were then placed in desiccator containing saturated salt solutions, and the leads passed through the rubber stopper (bung) on the top of the desiccator, connected to a special designed box containing a set of resistors to complete full bridges. The output voltage from these bridges were connected to a data logger to record the strains at chosen time intervals. The test was terminated when the strains became constant as shown in Figure 3(*a*), (*b*), and (*c*). Plotting the swelling strains at equilibrium normal and parallel to bedding planes at various water activities (relative humidity) yields a straight line.

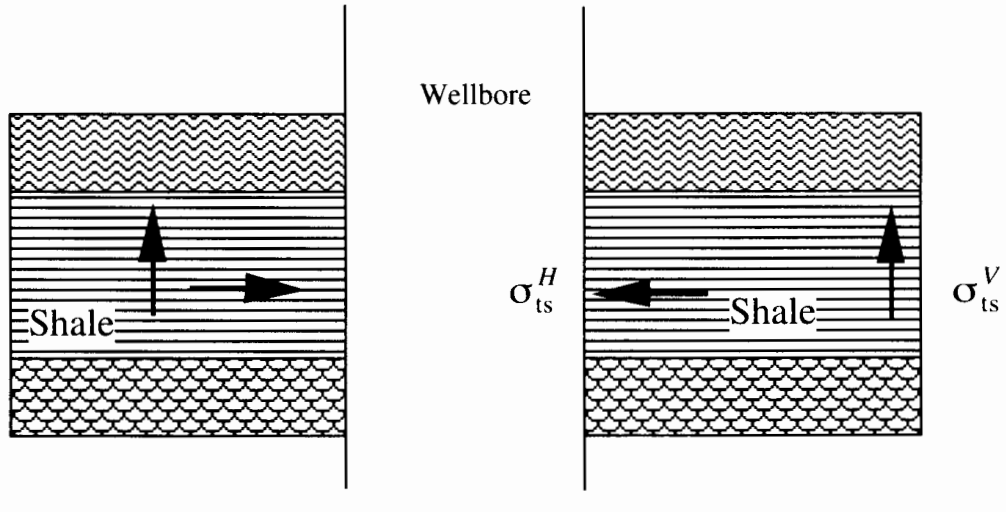

Figure 2. Total Swelling Stress Direction in Shale Formations.

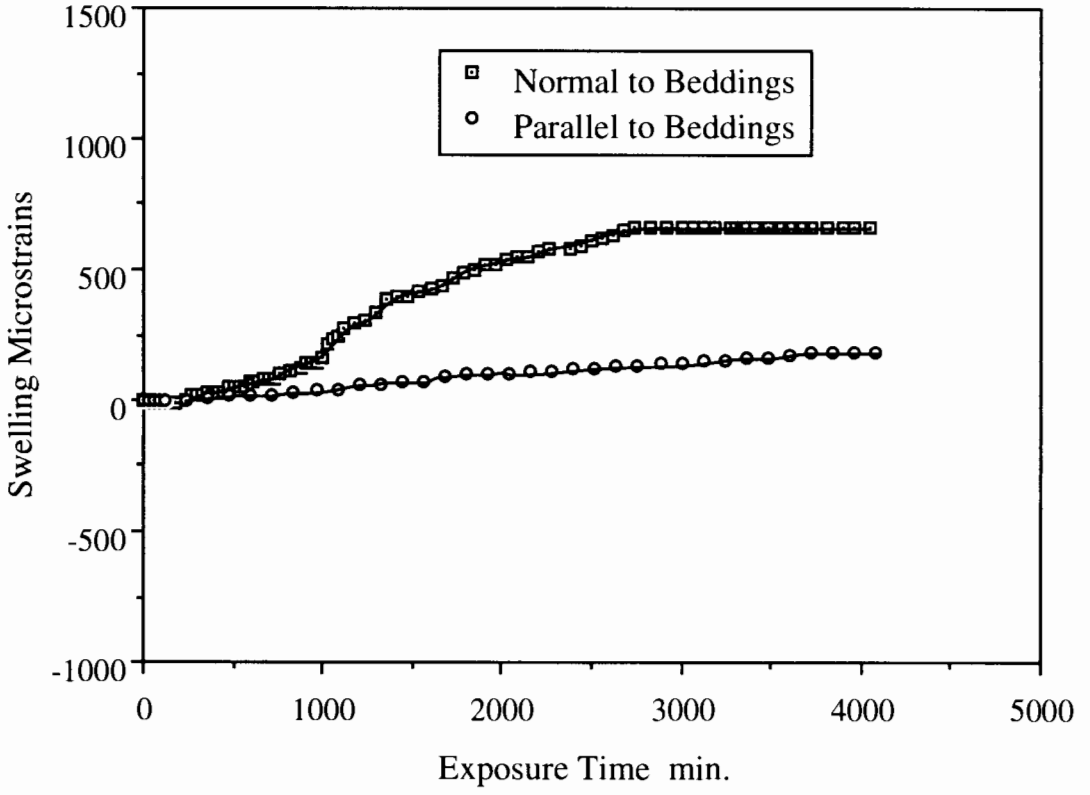

Figure 3(a). *Anisotropy Factor Determination for Intact FMS-Shale when Exposed to at 30% Relative Humidity.*

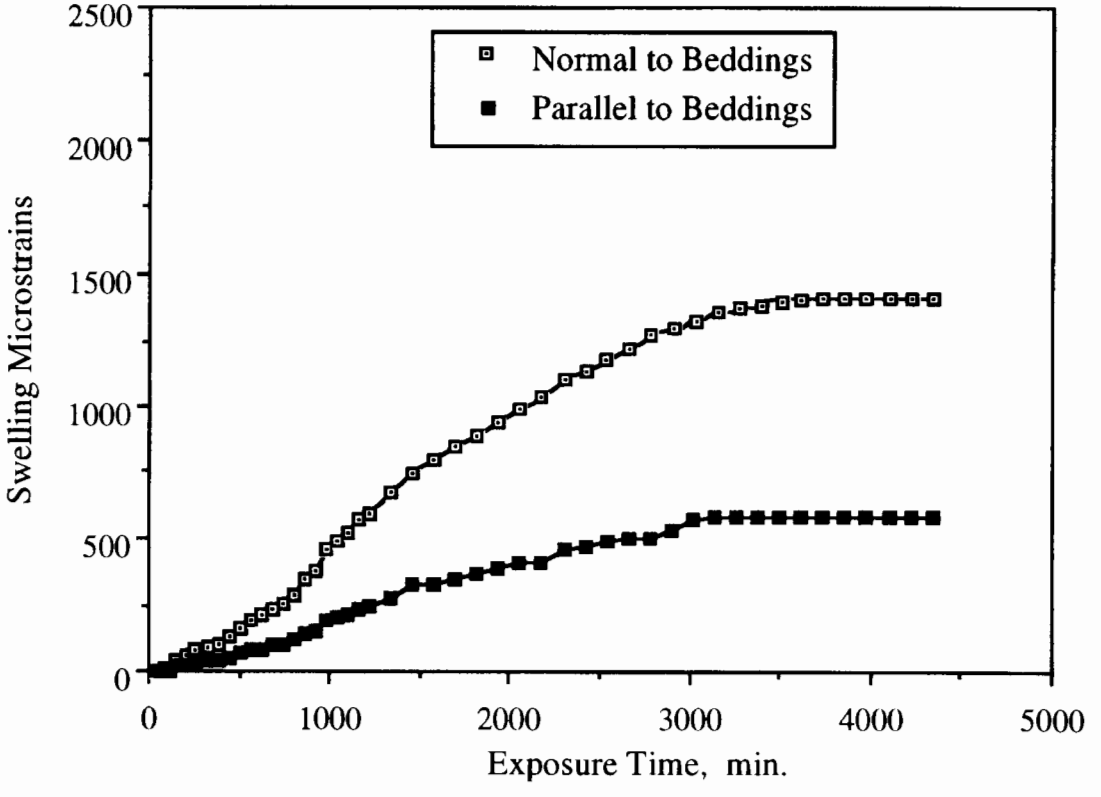

Figure 3(b). *Anisotropy Factor Determination for Intact FMS-Shale when Exposed to Relative Humidity of 75.5%.*

The anisotropy factor equal to the slope of the straight line as shown in Figure 4:

$$\Psi = \left(\frac{\varepsilon_H}{\varepsilon_V} \right) . \tag{10}$$

From these tests, it can be seen that the lateral strains are smaller than vertical ones. This difference in magnitude between horizontal and vertical swelling strains is believed to be due to high shale density (2.65 g cm^{-1}) and alignment of clay minerals during sedimentation. The following conclusions can be drawn out from this test. The shale is considered anisotropic when the anisotropy factor is greater or less than unity. From this test it was found that for a certain shale type, a unique anisotropy factor was measured regardless of humidity magnitude. This technique can help in determining the anisotropy factor of sensitive shales without affecting their mechanical properties. It is clear from this technique that, when shale specimen adsorbed water up to a level above its initial moisture content, swelling strains in both directions normal and parallel to bedding planes are generated. These strains are able to produce or enhance microfractures or/and separate the sample through its bedding.

4.3. Shale Adsorption Isotherm

Shale Adsorption Isotherm which relates the amount of clay in a shale to its moisture content was established for the tested shale. This was performed by placing a sample from the shale under consideration in a range of water activities (relative humidity). This was achieved by placing the shale inside vacuum desiccators containing saturated salt solutions in their shallow base. Samples inside these desiccators will either gain or lose moisture. The Adsorption Isotherm then established by plotting the gained moisture content at equilibrium *versus* salt water activity as shown in Figure 5.

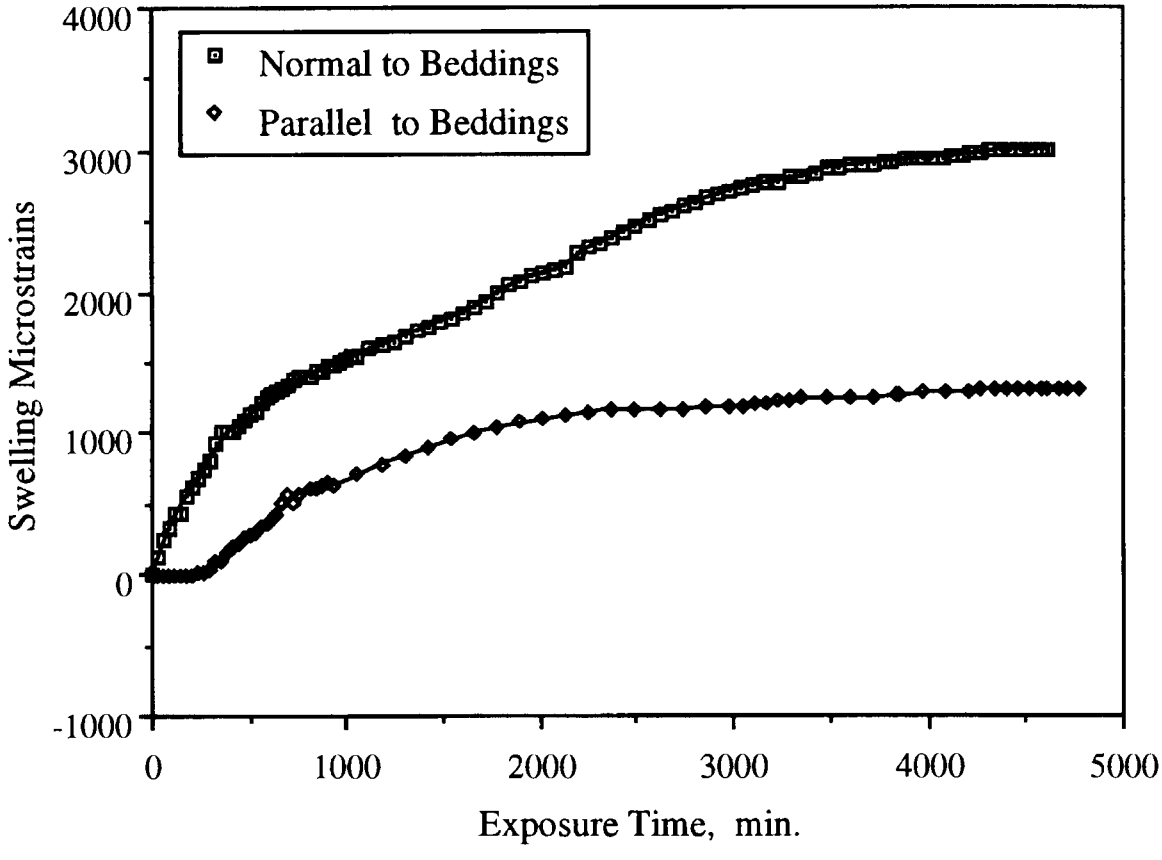

Figure 3(c). Anisotropy Factor Determination for Intact FMS-Shale when Exposed to at 96% Relative Humidity.

4.4. Swelling Strains–Moisture Content Relationship

When shale moisture content is altered, its dimensions may change due to this alteration. This change in shale dimensions in turn will produce swelling strains in its boundaries. Each cylindrical shale specimen was attached with two strain gauges in order to measure any change in sample dimensions in both directions normal and parallel to bedding planes. The strain gauged samples were then placed in a high relative humidity desiccators, and swelling strains in both direction were recorded using a data logging system. When the sample is placed in the desired desiccator, strain gauges leads are connected to the interface box, then to the data logger, after that, the desiccator is evacuated using vacuum pump. Sample weight is measured at specified time intervals by opening the desiccator and weighing the sample using electronic balance. When there is no change in sample weight, test was terminated. Figure 6 represents the relationship between moisture content and swelling strains for FMS-shale obtained by averaging the results of three experimental runs.

4.5. Measurement of Shale Swelling Strains

Cylindrical shale specimens of 1.5″×3.25″ dimensions were strain gauged with diametrically opposed pairs of bounded 120 Ω active vertical and horizontal electrical resistance strain gauges in a 90° rosette. The specimen was then placed in a triaxial cell and loaded with a dedicated loading arrangement (Figure 7) and subjected to fluid invasion (9.5% by volume NaCl solution) at 3.45 MPa over an extended period of time until equilibrium was reached, *i.e.* swelling strains were stabilized; and then the tests were terminated [9] as shown in Figure 8.

4.6. Conversion of Shale Swelling Strains to Swelling Stresses

The measured vertical and lateral swelling strains generated due to shale–fluid interaction were converted to swelling stresses using the following technique as shown in Table 1:

(*i*) For any specific period of time the recorded swelling strains normal to beddings can be read from Figure 8 which represents experimental time–strain relationship.

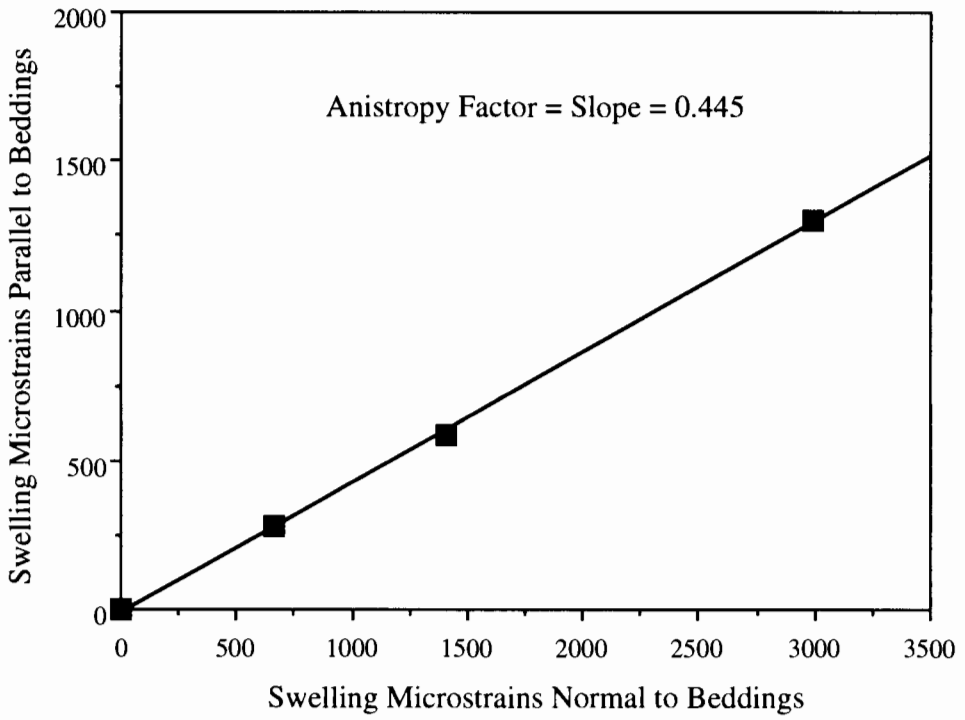

Figure 4. Relationship Between Swelling Microstrains Normal and Parallel to Beddings for FMS-Shale when Exposed to Various Relative Humidity.

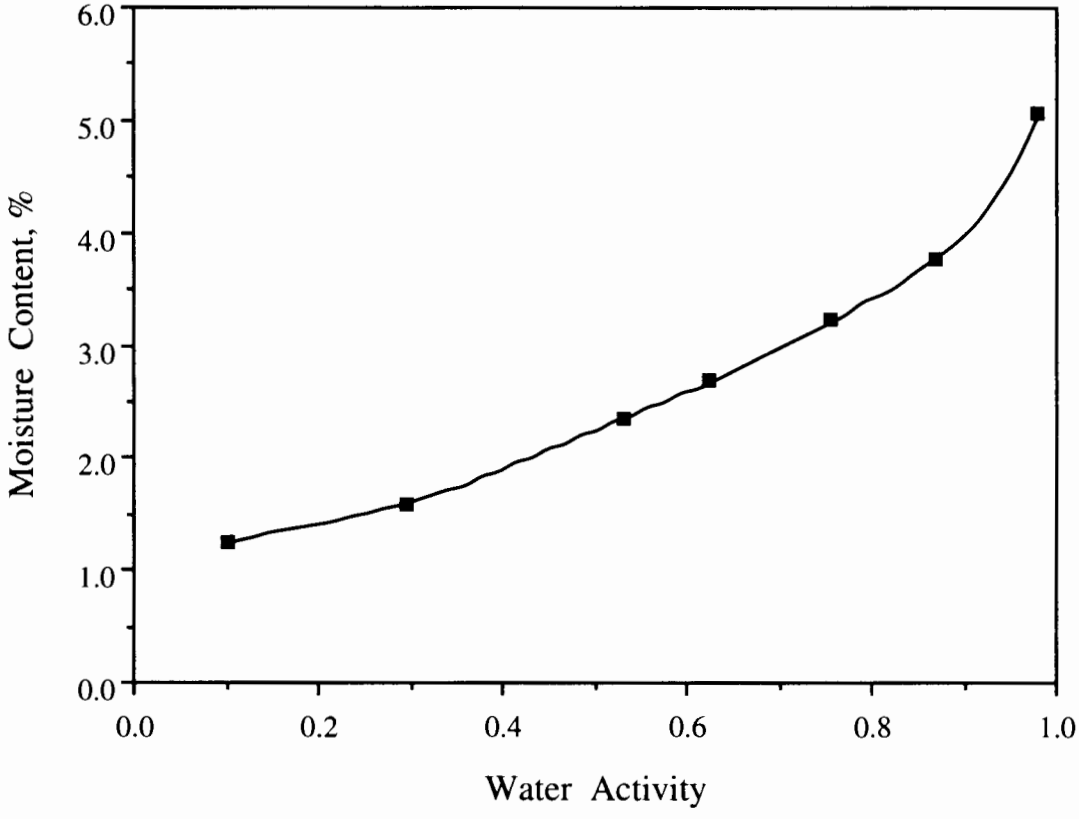

Figure 5. Adsorption Isotherm for FMS-Shale.

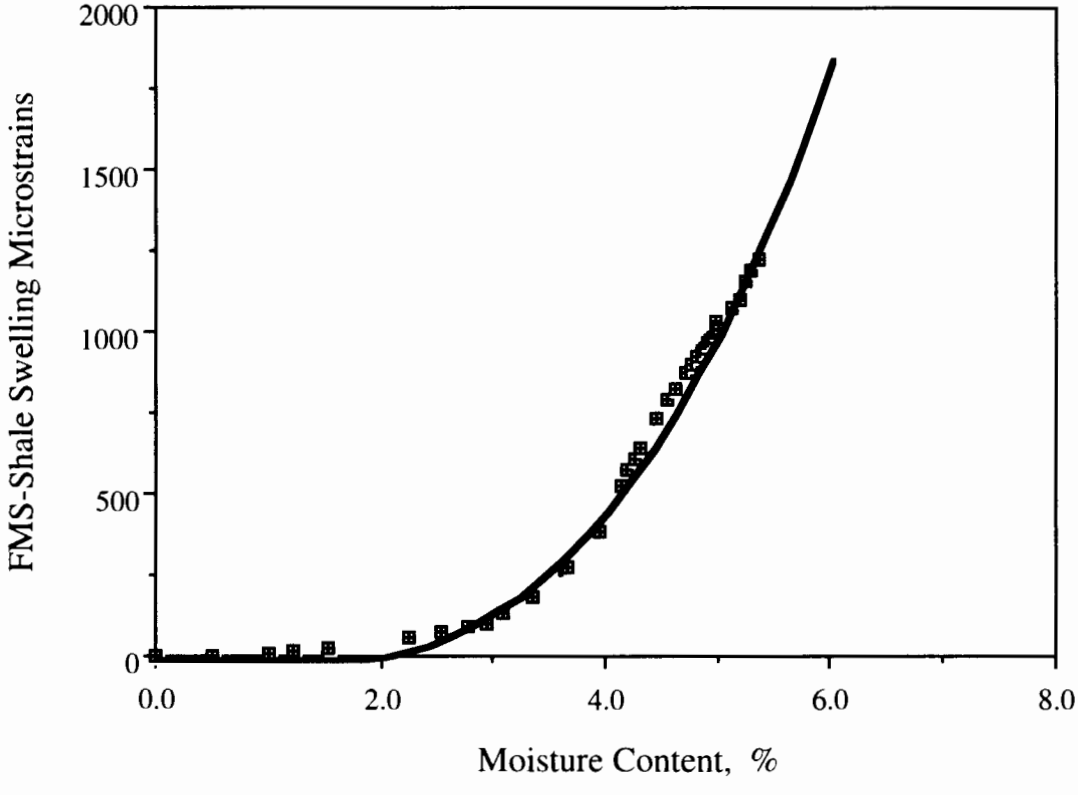

Figure 6. Relationship Between Moisture Content and Swelling Microstrains for FMS-Shale.

(*ii*) The computed swelling strain in step (*i*) is used to obtain the corresponding moisture content from Figure 6.

(*iii*) Moisture content read in step (*ii*) is used to compute the corresponding water activity from Figure 5 *i.e.* the Adsorption Isotherm.

(*iv*) The resulted water activity obtained in step (*iii*) is substituted in the adsorptive pressure law [10, 11] to obtain the experimental swelling stresses as follows:

$$P = \left[\frac{RT}{\bar{V}}\right] * \ln\left[a_w\right]. \tag{11}$$

Table 1 shows the conversion process of the experimental swelling strains to swelling stresses, as explained above.

Table 1. Conversion of FMS-Shale Swelling Strains to Swelling Stresses.

Exposure Time	Swelling Strains	Moisture Content	Shale Water Activity	Experimental Swelling Pressure	Shale Adsorptive Pore Pressure	Net Swelling Pressure
h	$\times 10^{-6}$	% by Weight		MPa	MPa	MPa
1	338	3.677	0.852	–22.33	–22.64	0.31
7	422	3.902	0.883	–17.28	–22.64	5.36
52	472	4.023	0.898	–15.1	–22.64	7.54

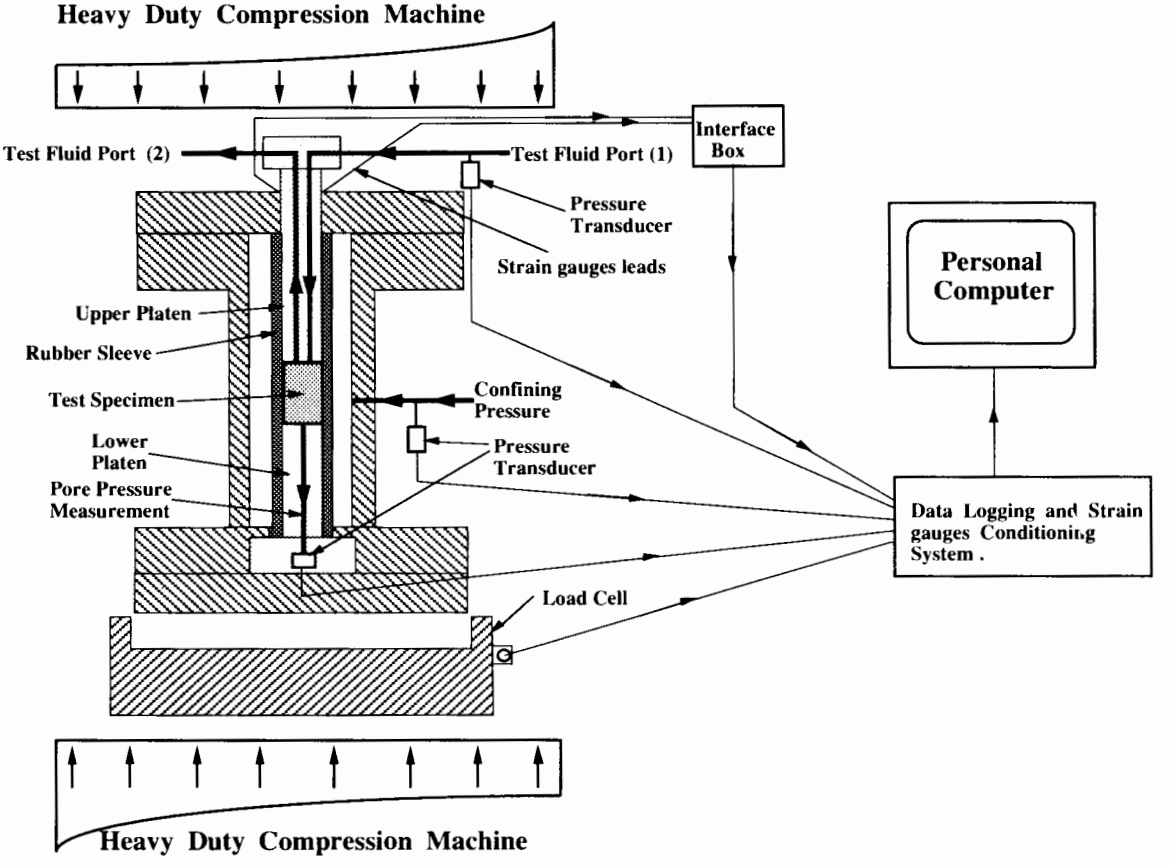

Figure 7. Schematic Diagram of the Triaxial Cell and Data Logging System.

4.7. Measurement of Shale Failure Criterion

The 1.5″×3.25″ shale cylindrical specimens were placed in a Hoek-type triaxial cell rated to 70 MPa, providing radial confinement by means of hydraulic oil acting on a synthetic membrane jacketing the specimen, this confining pressure being developed by means of a servo-controlled hydraulic intensifier. Axial load was provided by a stiff testing machine as shown in Figure 9(*a*) and (*b*). Ten specimens were used to establish the Mohr circles required to obtain the locus of the failure envelope. All of these ten shale specimens has zero moisture content *i.e.* zero pore pressure. On the other hand, failure criteria for hydrated shales were determined by placing shale specimens inside a specially designed triaxial cell and the conditions shown in Table 2 were applied. When swelling strains were stabilized the axial load were increased until failure was recorded. Failure data obtained from triaxial tests for both natural intact (moisture content = 0, *i.e.* zero pore pressure) and hydrated shale specimens (a_w = 0.85) are shown in Table 3.

5. RESULTS AND DISCUSSION

Table 4 shows how the triaxial data of intact shale samples is combined with swelling data to predict the change in shale mechanical properties while Figures 10 to 13 show the failure criteria of tested shale samples under different

Table 2. Testing Conditions for FMS-Shale Swelling Tests.

Drilling Fluid Type	=	9.5% by volume NaCl Solution
Drilling Fluid Water Activity	=	0.95
Shale Type	=	FMS-Shale
Shale Water Activity	=	0.85
Test Fluid Injection Pressure	=	3.45 MPa
Confining Pressure at all Swelling Tests	=	6.895 MPa
Axial Load at all Swelling Tests	=	7.85 kN
Dimensions of Shale Specimens	=	1.5″ x 3.25″

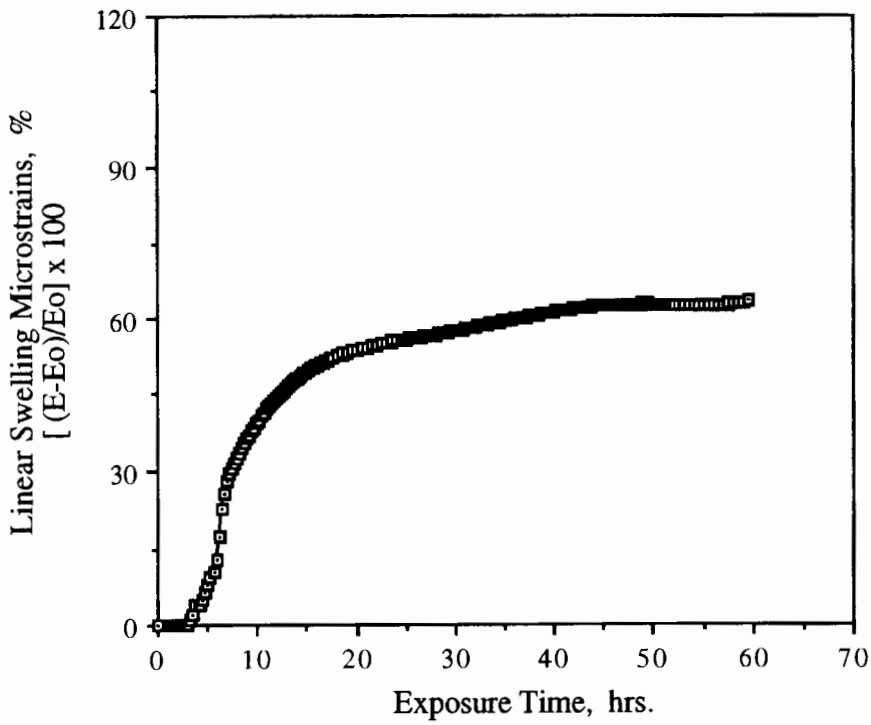

Figure 8. Experimental Vertical Swelling Microstrains Generated in FMS-Shale when Exposed to 9.5% by Volume NaCl Solution.

magnitudes of swelling stresses. Figure 14 shows a comparison between natural intact and reacted (hydrated) shale failure criteria with those obtained using the modified Mohr–Coulomb failure criterion. Although more tests are required to assess this model, it is provided reasonable predictions of shale strength reduction. It is clear that shale strength decreases as the total swelling stress increases. Shale apparent cohesion decreases as the swelling stresses increases. This is due to the increase in the amount of invasion fluid which is weakened the bonds between clay particles and lubricate the existing microfractures as well as the natural bedding planes. The angle of internal friction was independent of swelling stresses magnitude as shown in Figure 15. These results are in complete agreement with Hayatdavoudi *et al.* [5]. Therefore Equation (8) can be written in the following form:

$$\tau_f = \tau_o^* + \tan(\phi)\,, \tag{12}$$

where:

$$\begin{cases} \tau_o^* = \tau_o & \text{for } \sigma_{ts} = 0 \rightarrow \Delta MC = 0 \\ \tau_o^* = \tau_o - [\sigma_{ts} \tan(\phi)] & \text{for } \sigma_{ts} > 0 \rightarrow \Delta MC > 0 \end{cases}.$$

Table 3. Experimental Triaxial Failure Data of FMS-Shale Samples Reacted with 9.5% by Volume NaCl Solution for Various Exposure Intervals (at the End of Tests).

Case no.	Confining Pressure σ_3, MPa	Axial Stress at Failure σ_1, MPa	Remarks
1	6.895	30.67	Natural sample with moisture content = 0
2	6.895	28.96	After 1 hour exposure to 9.5% by volume NaCl solution
3	6.895	26.36	After 7 hours exposure to 9.5% by volume NaCl solution
4	6.895	23.62	After 52 hours exposure to 9.5% by volume NaCl solution

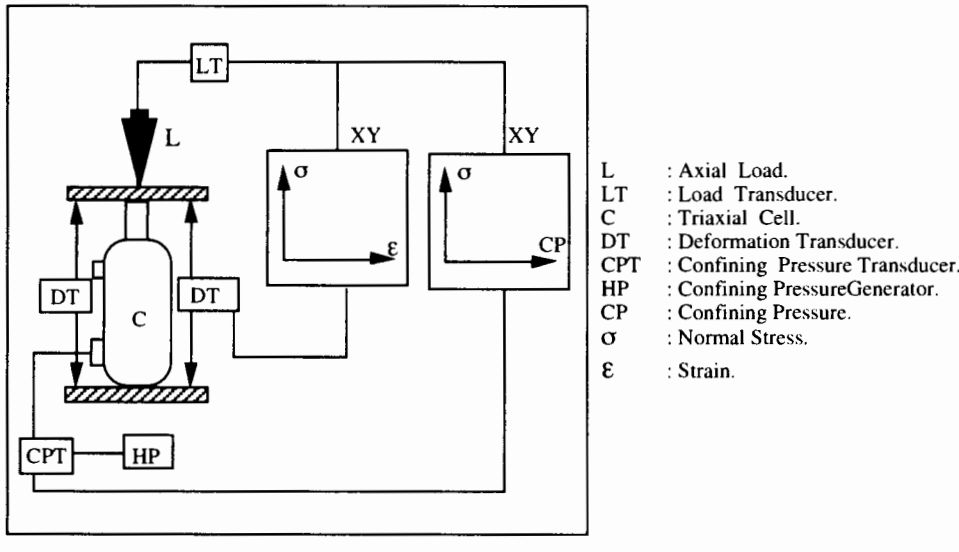

Figure 9(a). *Schematic Diagram of Equipment Used to Measure Shale Failure Criteria.*

Table 4. Calculations of Triaxial Failure Data for the Modified Mohr–Coulomb Failure Criterion for FMS-Shale when Exposed to 9.5% by Volume NaCl Solution at Various Exposure Times.

Case -1-		Case -2-		Case -3-		Case -4-	
Measured triaxial failure data for FMS-shale at its natural intact conditions		Calculated triaxial failure data for FMS-shale when exposed to 9.5% by volume NaCl solution Initial moisture content = 3.67 Initial water activity = 0.85					
Initial moisture content = 0 Initial water activity = 0 No swelling test $F_{anis} = 0.45$ σ_{ts}^{V} =Experimentally determined $\sigma_{ts}^{H} = F_{anis} * \sigma_{ts}^{V}$ ..... $\sigma_{ts}^{H} = 0$ MPa $\sigma_{ts}^{V} = 0$ MPa		Final moisture content = 3.677 Final water activity = 0.852 Swelling test duration = 1 hour $F_{anis} = 0.45$ σ_{ts}^{V} = Experimentally determined $\sigma_{ts}^{H} = F_{anis} * \sigma_{ts}^{V}$ ..... $\sigma_{ts}^{H} = 0.14$ MPa $\sigma_{ts}^{V} = 0.31$ MPa		Final moisture content = 3.912 Final water activity = 0.883 Swelling test duration = 7 hours $F_{anis} = 0.45$ σ_{ts}^{V} = Experimentally determined $\sigma_{ts}^{H} = F_{anis} * \sigma_{ts}^{V}$ ..... $\sigma_{ts}^{H} = 2.30$ MPa $\sigma_{ts}^{V} = 5.36$ MPa		Final moisture content = 4.023 Final water activity = 0.893 Swelling test duration = 52 hours $F_{anis} = 0.45$ σ_{ts}^{V} = Experimentally determined $\sigma_{ts}^{H} = F_{anis} * \sigma_{ts}^{V}$ ..... $\sigma_{ts}^{H} = 3.26$ MPa $\sigma_{ts}^{V} = 7.54$ MPa	
σ_1 MPa	σ_3 MPa	$\bar{\sigma}_3 = \left[\sigma_3 - \sigma_{ts}^{H}\right]$ MPa	$\bar{\sigma}_1 = \left[\sigma_1 - \sigma_{ts}^{V}\right]$ MPa	$\bar{\sigma}_3 = \left[\sigma_3 - \sigma_{ts}^{H}\right]$ MPa	$\bar{\sigma}_1 = \left[\sigma_1 - \sigma_{ts}^{V}\right]$ MPa	$\bar{\sigma}_3 = \left[\sigma_3 - \sigma_{ts}^{H}\right]$ MPa	$\bar{\sigma}_1 = \left[\sigma_1 - \sigma_{ts}^{V}\right]$ MPa
2.00	17.53	1.86	17.22	–0.304	12.18	–1.26	9.95
3.00	22.00	2.86	21.89	0.700	16.64	–0.26	14.41
4.00	25.00	3.86	24.68	1.700	19.64	0.74	17.41
5.00	26.30	4.86	25.99	2.700	20.94	1.74	18.71
6.00	27.41	5.86	27.10	3.700	22.05	2.74	26.72
7.00	30.70	6.86	30.39	4.700	25.24	3.74	23.11
8.00	32.44	7.86	32.13	5.600	27.08	4.74	24.86
9.00	34.20	8.86	33.89	6.700	28.84	5.74	26.62
10.00	36.00	9.86	35.68	7.700	30.65	6.74	28.41
11.00	39.50	10.86	39.18	8.700	34.14	7.74	31.91

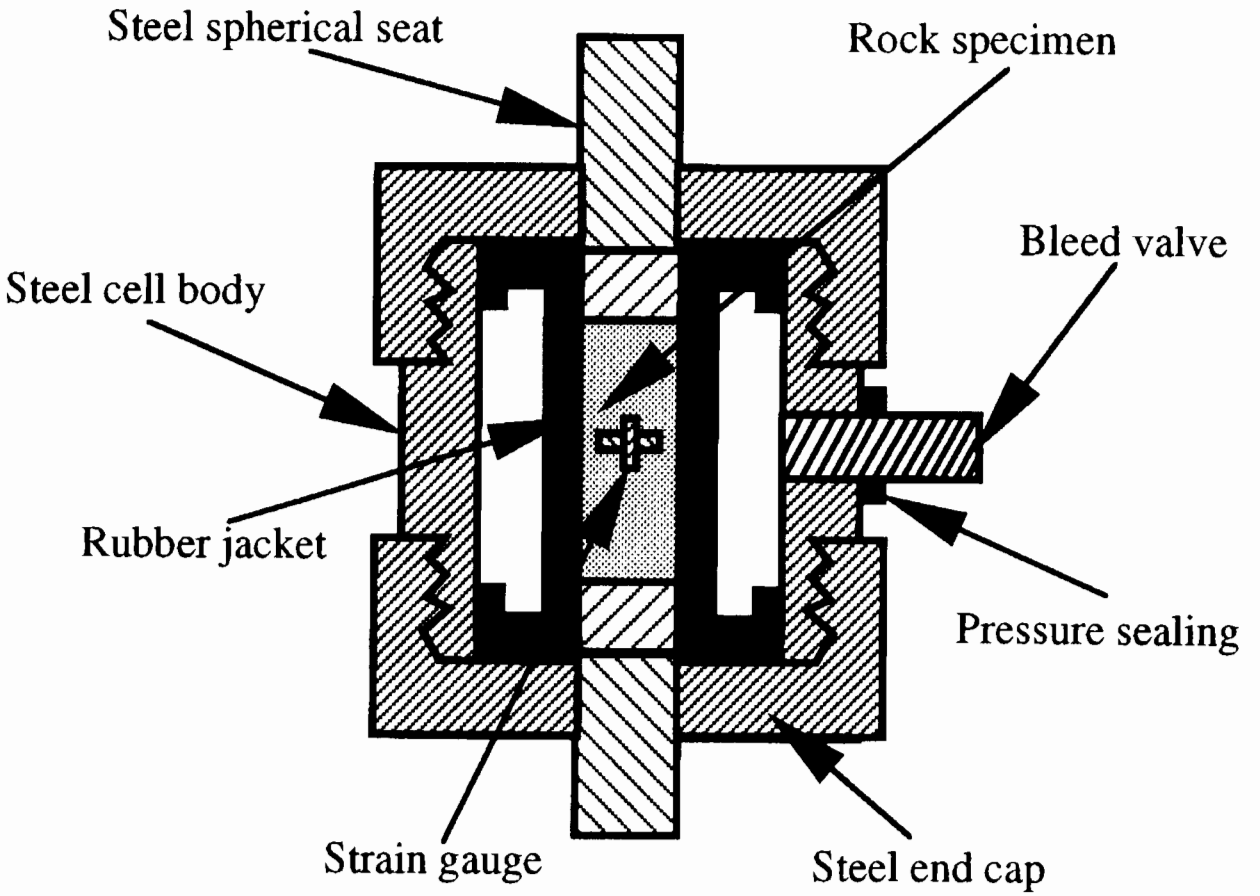

Figure 9(b). Schematic Diagram of Hoek–Franklin Triaxial Cell.

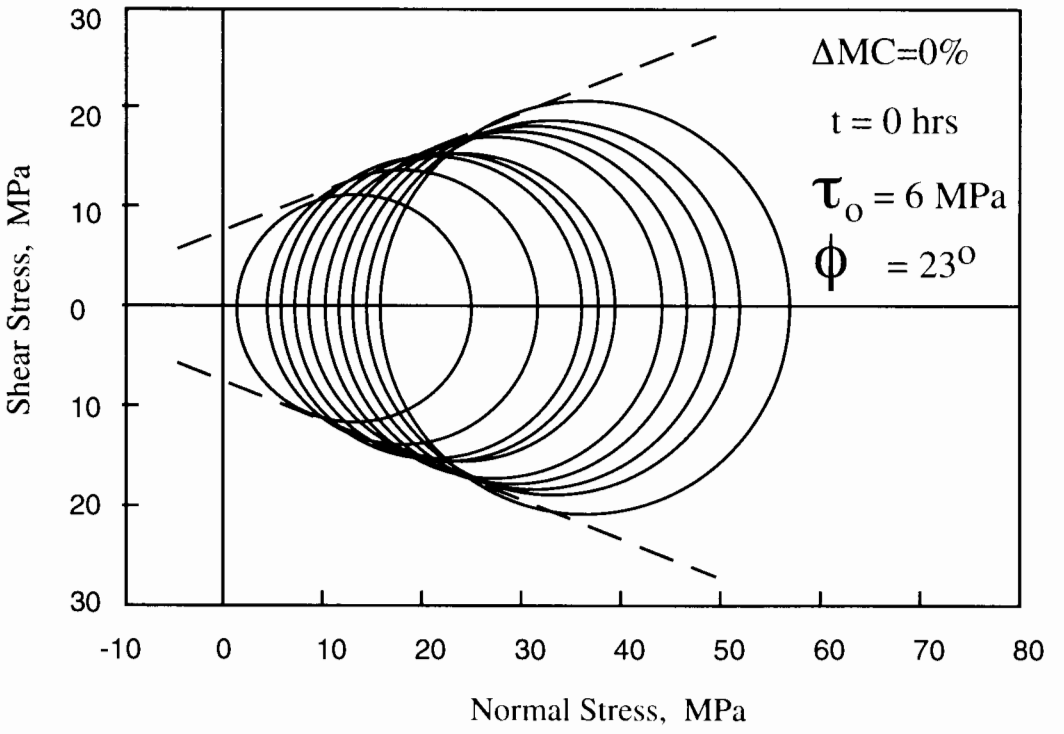

Figure 10. Mohr–Coulomb Failure Criterion for Natural Intact FMS-Shale.

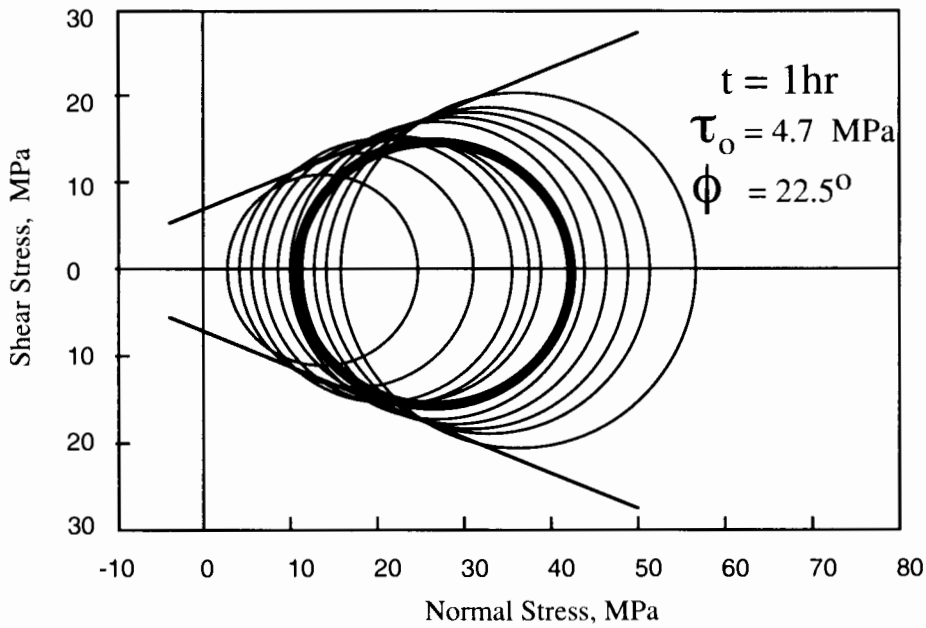

Theoretically Derived Mohr Circles for Reacted Samples.

Experimentally Derived Mohr Circle for Reacted Sample.

Figure 11. Mohr–Coulomb Failure Criterion for FMS-Shale After 1.0 hour of Interaction with 9.5% NaCl Solution.

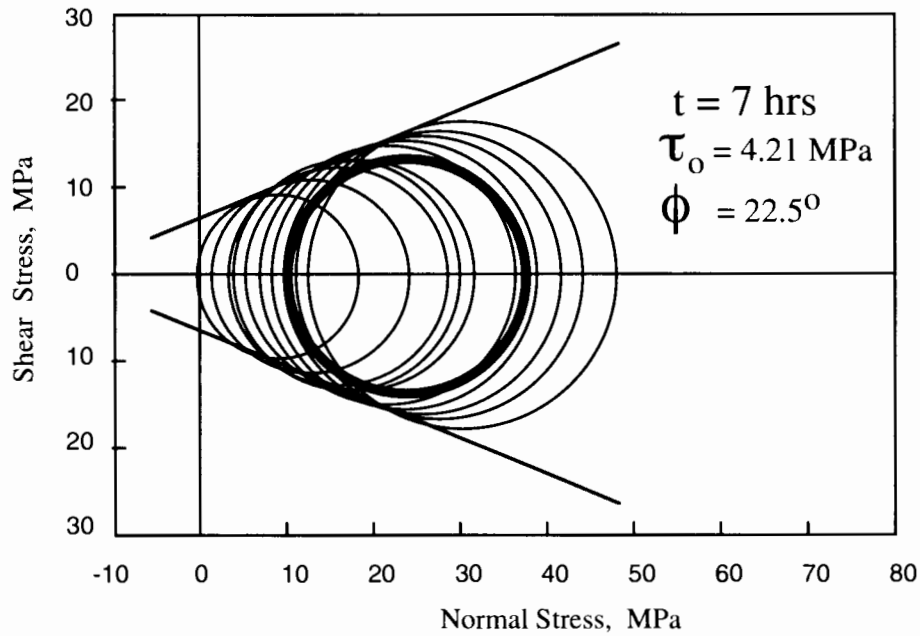

Theoretically Derived Mohr Circles for Reacted Samples.

Experimentally Derived Mohr Circle for Reacted Sample.

Figure 12. Mohr–Coulomb Failure Criterion for FMS-Shale After 7 hours of Interaction with 9.5% NaCl Solution.

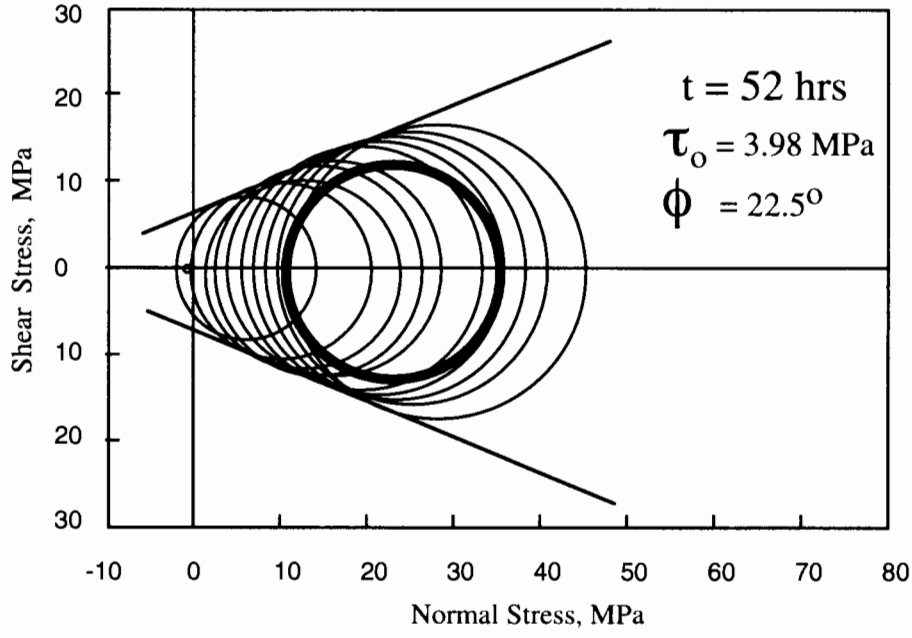

Theoretically Derived Mohr Circles for Reacted Samples.

Experimentally Derived Mohr Circle for Reacted Sample.

Figure 13. Mohr–Coulomb Failure Criterion for FMS-Shale After 52 hours of Interaction with 9.5% NaCl Solution.

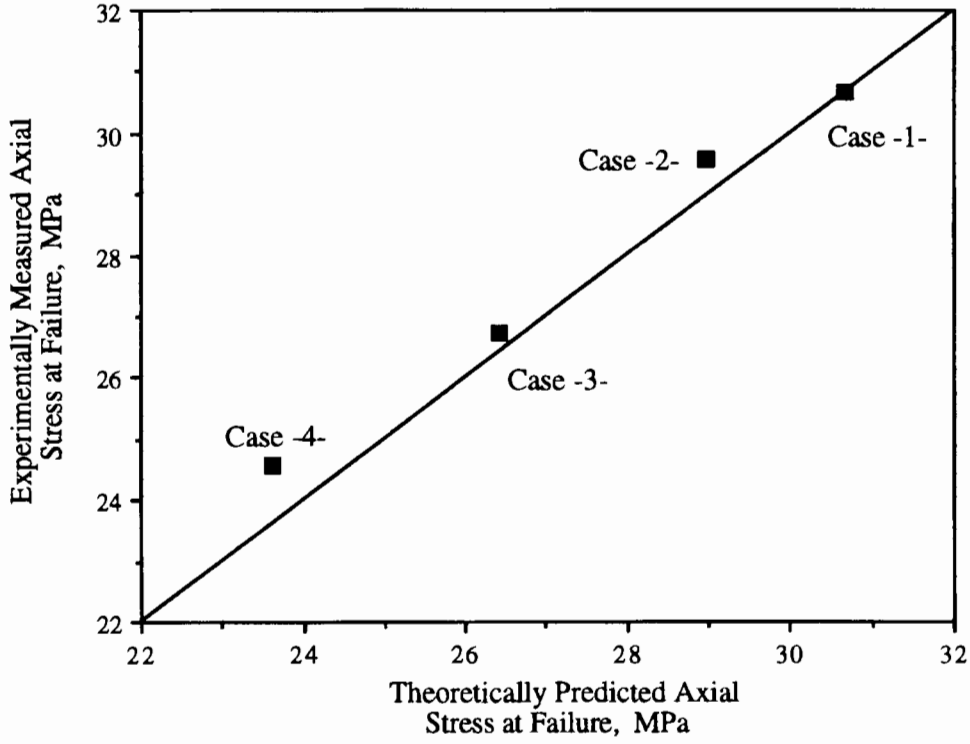

Figure 14. Comparison Between Experiment and Theoretical Axial Stress at Failure for FMS-Shale.

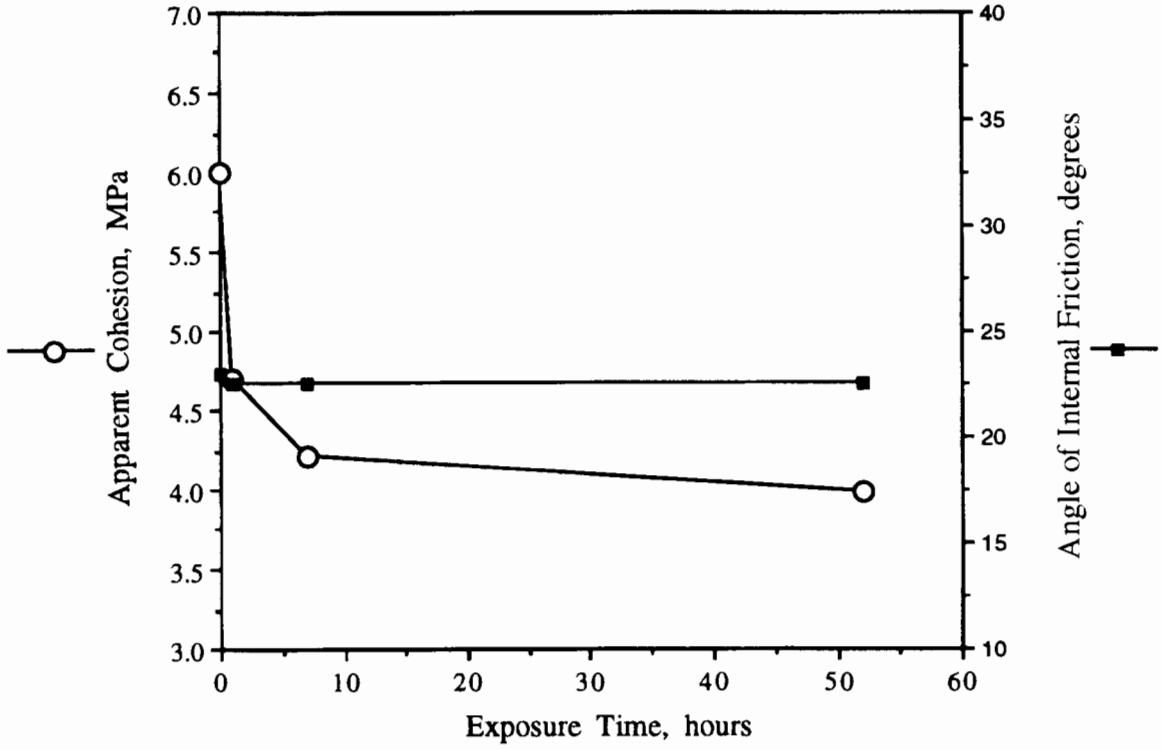

Figure 15. Effect of Swelling Stresses (Exposure Time) on Shale Frictional Properties.

6. CONCLUSIONS

(*i*) Mohr–Coulomb failure criterion was modified to account for the swelling stresses generated due to shale–fluid interaction.

(*ii*) Swelling strains were measured experimentally under realistic stresses and were found to be function of moisture front advance *i.e.* function of exposure time.

(*iii*) Shale apparent cohesion was decreased when the swelling stresses were increased, while the angle of internal friction was found to be independent of swelling stresses magnitude.

(*iv*) The modified criterion represents a new effective method which can be applied to predict the reduction in shale strength due to the incompatibility with drilling fluid, hence borehole instability can be avoided.

(*v*) Shale strength was reduced when mud filtrate front was advanced away from the wetted end of test sample. This process was perfectly described by the modified failure criterion.

7. NOMENCLATURE

a_w = Water activity.
F_{anis} = Shale anisotropy factor.
P = Hydration Stress.
P_p = Pore fluid pressure.
R = Gas constant.
T = Absolute temperature.
$\bar{V}$ = Pure water partial molar volume.
β = Angle of obliquity, degrees.

ϕ = Angle of internal friction.
ΔMC = Net gain in moisture.
τ_f = Shear stress at failure.
τ_o = Apparent cohesion of rock.
σ = Normal stress.
σ^i_{eff} = Effective stress in i-direction.
σ^i = Total Stress in i-direction.
σ^i_{hyd} = Hydration stress in i-direction.
σ_{ts} = Total swelling stress.
σ^V_{ts} = Total swelling stress normal to bedding planes.
σ^H_{ts} = Total swelling stress parallel to bedding planes.
σ_{os} = Osmotic swelling stress.
σ_{sur} = Surface swelling stress.
Ψ = Anisotropy coefficient.
ε_H = Swelling strains parallel to bedding planes.
ε_V = Swelling strains normal to bedding planes.

REFERENCES

[1] F. Erling, *et al.*, *Petroleum Related Rock Mechanics*. Amsterdam: Elsevier Scientific Publishers, 1992, 338p.

[2] H. C. H. Darley, "A Laboratory Investigation of Borehole Stability", *Journal of Petroleum Technology*, 1969, pp. 883–892.

[3] A. Onaisi, C. Durand, and A. Ardibert, "Role of Hydration State of Shales in Borehole Stability", *Eurock' 94, Balkema*, pp. 275–284, ISBN 90 5410 502.

[4] J. C. Jaeger and N. G. W. Cook, *Fundamentals of Rock Mechanics, 3rd edn*. London: Chapmen and Hall, 1979.

[5] A. Hayatdavoudi and E. Apende, "A Theoretical Analysis of Wellbore Failure and Stability in Shales", *Rock Mechanics: Key to Energy Production, 27th Symposium for Rock Mechanics, Tuscaloosa, Alabama, U.S.A.*, June 1986, pp. 571–579.

[6] G. M. Bol and W. Sau-Wai, "Borehole Stability in Shales", *SPE 24975 European Petroleum Conference, Cannes, France*, 1992.

[7] M. E. Chenevert, "Diffusion of Water and Ions into Shales", in *Rock at Great Depth*. Rotterdam: Balkema, 1990, pp. 1177–1184, ISBN 9061919754.

[8] H. Yew Ching, M. E. Chenevert, L. Wang Chein, and S. O. Osisanya, "Wellbore Stress Distribution Produced by Moisture Adsorption", *SPE Drilling Engineering*, December 1990, pp. 311–316.

[9] Musaed Naser J. Al-Awad, "Physico–Chemical Modelling of Shale-Drilling Fluid Interaction and Its Application to Borehole Stability Studies", *Unpublished Ph.D. Thesis, Department of Petroleum Engineering, Heriot-Watt University, Edinburgh, U.K.*, 1994.

[10] L. Schmitt, T. Forsans, and F. J. Santarelli, "Shale Testing and Capillary Phenomena", *Int. J. Rock Mech. Min. Sci. & Geomech. Abstr.*, **31(5)** (1994), pp. 411–427.

[11] M. E. Chenevert, "Adsorptive Pore Pressure in Argillaceous Rocks", *Proc. of the 11th. Symp. on Rock Mech., U. of California, Berkeley*, June 16–19, 1969.

Paper Received 2 January 1995; Revised 18 June 1995; Accepted 5 November 1995.